THE METHOD OF MICRO-UPSETTING IN UNEVEN TEMPERATURE DISTRIBUTION

Wojciech PRESZ

Warsaw University of Technology, Institute of Manufacturing Technologies, Warsaw, Poland, EU
w.presz@wip.pw.edu.pl

Abstract

A method of determining the plastic properties of the material under the conditions of microforming at elevated temperatures was presented. This involves performing the process of upsetting a cylindrical micro sample between flat tools of different temperatures. As a result of the heat flow in the volume of the sample the non-uniform temperature distribution is observed. It causes uneven distribution of deformations and a shape similar to the truncated cone is obtained. Based on the measurement of the sample side contour, FEM simulation of the process and the known temperature at several points of tooling it is possible to determine the dependence of the plastic resistance on the temperature within the given range. Dependence is derived from one experiment. This method is recommended for studies where the number of samples for analysis is limited. The method allows to quickly determine the temperature characteristics of a material. A sample analysis of selected bulk metallic glass was presented.

Keywords: Microforming, micro-upsetting, elevated temperature

1. INTRODUCTION

Along with the progressive miniaturization of electro-mechanical systems and opto-electro-mechanical systems, the need for precision-made metal elements with dimensions of less than 1 mm has been increasing for a longer time. Such elements can be successfully produced with the technology of metal forming [1], within which a new branch was created: microforming [2]. It was created when it was noticed that reducing the dimensions of deformed elements to approx. 1 mm, causes the incompatibility of previously used rules [3] (calculation of forming forces, friction forces, etc.) with reality [4]. Thus, the limit value was 1 mm, in relation to at least two dimensions of the object. The cause of observed discrepancies [5] was called the "size or scale effect" and the intensive (ongoing to date) work on explaining various aspects [6] of this phenomenon was started. The small dimensions of the components resulted in the construction of micro-tools [7] and tool systems [8] dedicated to microforming. Also some processes found a new solutions [9] possible to be carried out only in micro-scale [10]. The contact phenomena have also gained new aspects [11] dedicated to micro-parts and micro-tools [12]. The rapidly growing market of micro-mechanisms has also caused a rapidly growing number of new metallic materials [13] or compound billets [14] being developed with different composition, form [15] and structure [16]. To determine their plastic properties, the upsetting test for a whole range of conditions and requiring a large number of samples is relatively often used.

There appeared a need for quick methods of determining plastic features in the conditions of microforming, giving as much information as possible within a small number of experiments. The method presented below meets the above conditions.

2. THE CONCEPT OF THE MICRO-UPSETTING IN UNEVEN TEMPERATURE DISTRIBUTION METHOD

The method named „MUNUT“ consists in upsetting a cylindrical sample between flat anvils with different temperatures. The lower anvil has a temperature higher than the upper. This results in a "layered" temperature distribution. In relation to the dependence of the yield stress on temperature, each layer will have a different

yield point. After application of force - the same for each of the layers - the layers will deform plastically but to a different degree. Each of the layers is a circle with a different radius. As a consequence, a sample assumes the shape of a rotary body, see **Figure 1**. With the known temperature distribution, the method assumes the possibility of obtaining the dependence of the plasticizing stress on the temperature in the applied temperature interval.

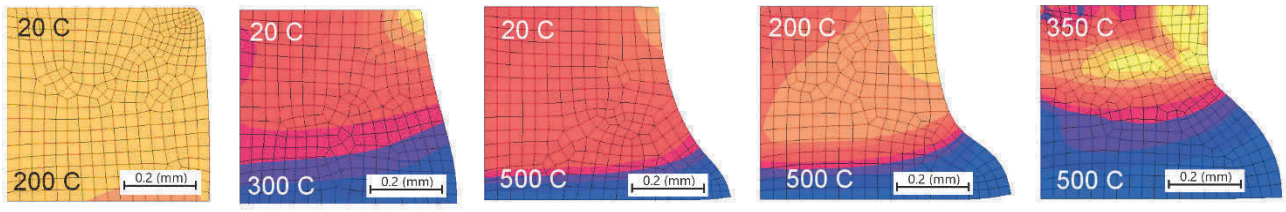

Figure 1 FEM modelling - von Mises stress: example of shapes obtained at different temperatures for the same material, same sample dimensions and same strain in the axial direction

2.1. Determining the distribution of stresses and strains

In each layer there is a complex state of stress and strain, but axially symmetrical. The method involves two experiments: one real "R" and one numeric "M". After applying the interpretation of the theory of mechanical similarity, we conclude on the basis of the results of the experiment with the object "M" on the physical quantities related to the object "R" - the material used in the "real" experiment.

Assuming cylindrical coordinates where *h* - distance from the base (mm), *r* - distance from the axis (mm), *φ* - angle (rad). Tension von Mises at the point in the object "R" is as follow.

$$\sigma_{H,\mathrm{R}}(h,r,\varphi) \tag{1}$$

where: $h \in (0, h_{\mathrm{b,R}})$, $r \in (0, r_{\mathrm{b,R,max}}(h)$ and $\varphi \in (0,\ 2\pi)$.

In the case of axial symmetry, the average equivalent stress $\bar{\sigma}_{H,\mathrm{R}}(h)$ and the average axial stress $\bar{\sigma}_{H,\mathrm{R}}(h)$ in the layer with the position *h* are (2) and (3), where $r_{b,\mathrm{R}}(h)$ is the outer radius of the layer with the location *h*.

$$\bar{\sigma}_{H,\mathrm{R}}(h) = \frac{1}{\pi \cdot r_b^2(h)} \cdot \iint_{0,0}^{r_{b,\mathrm{R}}(h),2\pi} \sigma_{\mathrm{H,R}}(h,r,\varphi)\mathrm{d}r\mathrm{d}\varphi \tag{2}$$

$$\bar{\sigma}_{1,\mathrm{R}}(h) = \frac{1}{\pi \cdot r_b^2(h)} \cdot \iint_{0,0}^{r_{b,\mathrm{R}}(h),2\pi} \sigma_{1,\mathrm{R}}(h,r,\varphi)\mathrm{d}r\mathrm{d}\varphi \tag{3}$$

The stress proportionality coefficient $\bar{\sigma}_{H,R}(h)$ and $\bar{\sigma}_{H,R}(h)$ in point (4) and its mean value in the layer defined as the quotient of the mean values of the functions in the layer (5) are introduced.

$$s_{\mathrm{R}}(h,r,\varphi) = \frac{\sigma_{H,\mathrm{R}}(h,r,\varphi)}{\sigma_{1,\mathrm{R}}(h,r,\varphi)} \tag{4}$$

$$\bar{s}_R(h) = \frac{\bar{\sigma}_{H,\mathrm{R}}(h,r,\varphi)}{\bar{\sigma}_{1,\mathrm{R}}(h,r,\varphi)} = \frac{\frac{1}{\pi \cdot r_b^2(h)} \cdot \iint_{0,0}^{r_{b\mathrm{R}}(h),2\pi} \sigma_{\mathrm{H,R}}(h,r,\varphi)\mathrm{d}r\mathrm{d}\varphi}{\frac{1}{\pi \cdot r_b^2(h)} \cdot \iint_{0,0}^{r_{b\mathrm{R}}(h),2\pi} \sigma_{1,\mathrm{R}}(h,r,\varphi)\mathrm{d}r\mathrm{d}\varphi} \tag{5}$$

The analogous explanation applies to equivalent strains $\varepsilon_{H,\mathrm{R}}$ and strain component $\varepsilon_{1,\mathrm{R}}$ and the introduction of the proportionality coefficient $w_{\mathrm{R}}(h,r,\varphi)$ and its average value $\bar{w}_{\mathrm{R}}(h,r,\varphi)$ in the position *h*, (6).

$$\bar{w}_{\mathrm{R}}(h) = \frac{\frac{1}{\pi \cdot r_{b,\mathrm{R}}^2(h)} \cdot \iint_{0,0}^{r_{b,\mathrm{R}}(h),2\pi} \varepsilon_{H,\mathrm{R}}(h,r,\varphi)\mathrm{d}r\mathrm{d}\varphi}{\frac{1}{\pi \cdot r_{b,\mathrm{R}}^2(h)} \cdot \iint_{0,0}^{r_{b,\mathrm{R}}(h),2\pi} \varepsilon_{1,\mathrm{R}}(h,r,\varphi)\mathrm{d}r\mathrm{d}\varphi} \tag{6}$$

The functions $\bar{s}_{\mathrm{R}}(h)$ and $\bar{w}_{\mathrm{R}}(h)$ allow to determine the average value of the equivalent stress $\bar{\sigma}_{H,\mathrm{R}}(h)$ and the average value of the equivalent strain $\bar{\varepsilon}_{H,\mathrm{R}}(h)$ in the layer with the position *h*, according to (7) and (8):

$$\bar{\sigma}_{H,\mathrm{R}}(h) = \bar{s}_{\mathrm{R}}(h) \cdot \bar{\sigma}_{1,\mathrm{R}}(h) \tag{7}$$

$$\bar{\varepsilon}_{H,\mathrm{R}}(h) = \bar{w}_{\mathrm{R}}(h) \cdot \bar{\varepsilon}_{1,\mathrm{R}}(h) \tag{8}$$

Similarly, in the case of simulation results, in which the object "M" is created, (9), (10).

$$\bar{s}_{\mathrm{M}}(h) = \frac{\frac{1}{\pi \cdot r_{b,\mathrm{M}}^2(h)} \cdot \iint_{0,0}^{r_{b,\mathrm{M}}(h),2\pi} \sigma_{\mathrm{H,M}}(\mathrm{h,r},\varphi)\mathrm{dr}\mathrm{d}\varphi}{\frac{1}{\pi \cdot r_{b,\mathrm{M}}^2(h)} \cdot \iint_{0,0}^{r_{b,\mathrm{M}}(h),2\pi} \sigma_{1,\mathrm{M}}(\mathrm{h,r},\varphi)\mathrm{dr}\mathrm{d}\varphi} \tag{9}$$

$$\bar{w}_{R}(h) = \frac{\frac{1}{\pi \cdot r_{b,\mathrm{R}}^2(h)} \cdot \iint_{0,0}^{r_{b,\mathrm{R}}(h),2\pi} \varepsilon_{\mathrm{H,R}}(\mathrm{h,r},\varphi)\mathrm{dr}\mathrm{d}\varphi}{\frac{1}{\pi \cdot r_{b,\mathrm{R}}^2(h)} \cdot \iint_{0,0}^{r_{b,\mathrm{R}}(h),2\pi} \varepsilon_{1,\mathrm{R}}(\mathrm{h,r},\varphi)\mathrm{dr}\mathrm{d}\varphi} \tag{10}$$

Then it is also possible to determine the average equivalent stresses and average equivalent strains based on the average axial components (11) and (12)

$$\bar{\sigma}_{H,\mathrm{M}}(h) = \bar{s}_{\mathrm{M}}(h) \cdot \bar{\sigma}_{1,\mathrm{M}}(h) \tag{11}$$

$$\bar{\varepsilon}_{H,\mathrm{M}}(h) = \bar{w}_{\mathrm{M}}(h) \cdot \bar{\varepsilon}_{1,\mathrm{M}}(h) \tag{12}$$

where: $h \in (0, h_{b,\mathrm{M}})$ and $\mathrm{r} \in (0, r_{\mathrm{b,M,max}}(h)$ and $\varphi \in (0,\ 2\pi)$

Comment on the theory of similarity: The term "similar" refers to the theory of similarity formulated by Buckingham and that the inference based on the study of the model of reality can be referenced to it only when the "similarity conditions" are met by the numbers of similarities defining the relations between the physical quantities of the model and reality

ARGUMENT: If the processes "R" and "M" are similar to the above worded similarity, then:

(a) the stress tensor ratios are the same,
(b) ratios of constituent strain tensors are the same,
(c) the proportionality of stress tensors may be different than strain tensors.

Comment on the thesis: In this analysed case, it was assumed that the similarity numbers are (13) and (14), which means that the outlines of both objects are consistent.

$$h_{b,\mathrm{R}} = h_{b,\mathrm{M}} \tag{13}$$

$$r_{\mathrm{b,R}}(\mathrm{h}) = r_{\mathrm{b,M}}(\mathrm{h}) \tag{14}$$

Consequently, the functions *s*(*h*) (5), (9) and *w(h)* (6), (10) in the case of reality and model are identical from which results (15) and (16).

$$\bar{\sigma}_{H,\mathrm{R}}(h) = \bar{s}_{\mathrm{M}}(h) \cdot \bar{\sigma}_{1,\mathrm{R}}(h) \tag{15}$$

$$\bar{\varepsilon}_{H,\mathrm{R}}(h) = \bar{w}_{\mathrm{M}}(h) \cdot \bar{\varepsilon}_{1,\mathrm{R}}(h) \tag{16}$$

This means that while meeting the similarity conditions, determining the functions $\bar{s}_{\mathrm{M}}(h)$ and $\bar{w}_{\mathrm{M}}(h)$ and on the basis of experiment, functions $\bar{\sigma}_{1,\mathrm{R}}(h)$ and $\bar{\varepsilon}_{1,\mathrm{R}}(h)$ are determined based on simulation results you can

designate (15) and (16) functions $\bar{\sigma}_{H,\mathrm{R}}(h)$ and $\bar{\varepsilon}_{H,\mathrm{R}}(h)$. The determination of the a fore mentioned functions boils down to an approximation of a set of values obtained on the basis of the mean values in the layer *i* in the "R" process (17), (18) and local values on circles *k* in the layer *j* in the "M" processes. The average values of stresses and strains in the "R" process and deformations are in accordance with (17), (18) and They are determined on the basis of measured force and profile measurements, see **Figure 2**.

$$\bar{\sigma}_{\mathrm{l},i,\mathrm{R}}(h_i) = \frac{F_\mathrm{R}}{\mathrm{A}_i} = \frac{F_\mathrm{R}}{\pi \cdot r_{b,\mathrm{R},i}^2} \tag{17}$$

$$\bar{\varepsilon}_{1,i,\mathrm{R}}(h_i) = 2\left|ln\frac{r_{b,\mathrm{R},i}}{r_{b,\mathrm{R},0}}\right| \tag{18}$$

where: F_R - the force of the process in the final phase of it (N), $r_{0,\mathrm{R},i}$ - initial radius (mm), $r_{b,\mathrm{R},i}$ - the extreme radius (mm) in the layer *j*, *i*={0,1, …, n} and (*j, k*) =({0,1,2, … , m, }, {0,1,2, … , u}).

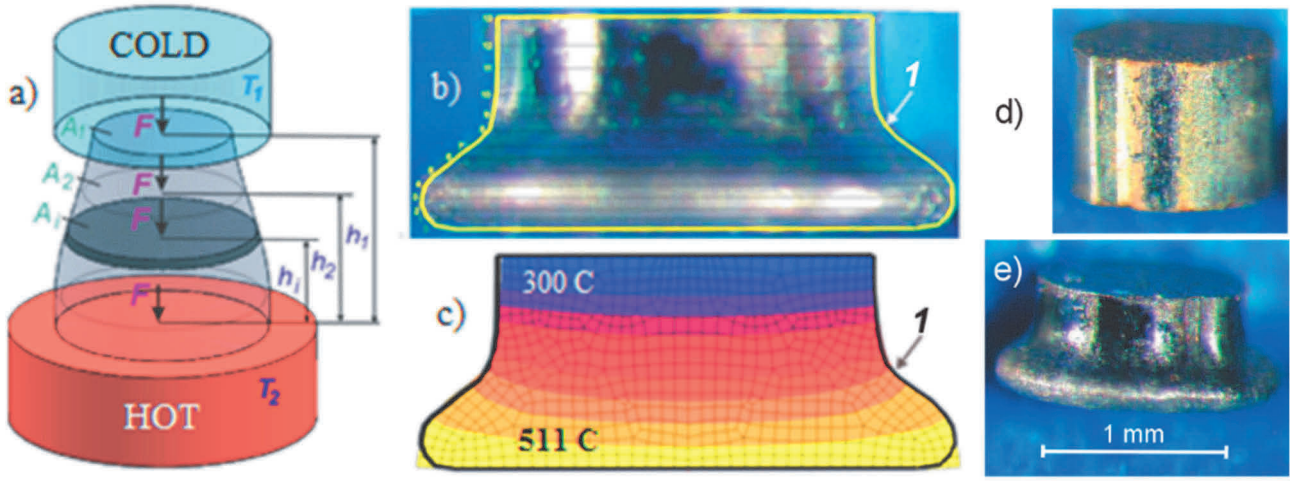

Figure 2 MUNUT method: a) principle, b) side view of specimen with outline "*1*", c) FEM result of deformed specimen with outline "*1*" and temperature distribution, d) specimen before deformation, e) specimen after deformation

The functions $\bar{s}_\mathrm{M}(h)$, $\bar{w}_\mathrm{M}(h)$ and $\bar{s}_{\mathrm{M},j}(h_j)$ are determined on the basis of the approximation of the values determined in the "M" model in the examined points (19):

$$\bar{s}_{\mathrm{M},j}(h_j) = \frac{\frac{1}{\pi r_{j,\mathrm{u}}^2}\sum_{k=0}^{\mathrm{u}}\frac{\sigma_{H,\mathrm{M},j,k+1}+\sigma_{H,\mathrm{M},j,k}}{2}\cdot 2\pi\cdot\frac{\left(r_{j,k+1}+r_{j,k}\right)}{2}\cdot\left(r_{j,k+1}-r_{j,k}\right)}{\frac{1}{\pi r_{j,\mathrm{u}}^2}\sum_{k=0}^{\mathrm{m}}\frac{\sigma_{1,\mathrm{M},j,k+1}+\sigma_{1,\mathrm{M},j,k}}{2}\cdot 2\pi\cdot\frac{\left(r_{j,k+1}+r_{j,k}\right)}{2}\cdot\left(r_{j,k+1}-r_{j,k}\right)} \tag{19}$$

The force of the process is constant (20):

$$\Lambda_j F_j = F_\mathrm{M} = \sum_{k=0}^{\mathrm{u}}\frac{\sigma_{1,\mathrm{M,j},k+1}+\sigma_{1,\mathrm{M,j,k}}}{2}\cdot 2\pi\cdot\frac{\left(r_{j,k+1}+rj,_k\right)}{2}\cdot\left(r_{j,k+1}-r_{j,k}\right) \tag{20}$$

$$\bar{s}_{M,j}(h_j) = \frac{1}{2r_u^2\cdot F_\mathrm{M}}\cdot\sum_{k=0}^{\mathrm{u}}(\sigma_{H,\mathrm{M},j,k+1}+\sigma_{\mathrm{H,M,j,k}})\cdot(r_{j,k+1}^2-r_{j,k}^2) \tag{21}$$

$$\bar{w}_{M,j}(h_j) = \frac{\frac{1}{\pi r_{j,\mathrm{u}}^2}\sum_{k=0}^{\mathrm{u}}\frac{\varepsilon_{\mathrm{E,M},j,k+1}+\varepsilon_{\mathrm{E,M},j,k}}{2}\cdot 2\pi\cdot\frac{\left(r_{j,k+1}+r_{j,k}\right)}{2}\cdot\left(r_{j,k+1}-r_{j,k}\right)}{\frac{1}{\pi r_{j,\mathrm{u}}^2}\sum_{k=0}^{\mathrm{u}}\frac{\varepsilon_{1,\mathrm{M},j,k+1}+\varepsilon_{1,\mathrm{M},j,k}}{2}\cdot 2\pi\cdot\frac{\left(r_{j,k+1}+r_{j,k}\right)}{2}\cdot\left(r_{j,k+1}-r_{j,k}\right)} = \sum_{k=0}^{\mathrm{u}}\frac{\varepsilon_{H,\mathrm{M},j,k+1}+\varepsilon_{\mathrm{E,M},j,k}}{\varepsilon_{1,\mathrm{M},j,k+1}+\varepsilon_{1,\mathrm{M},j,k}} \tag{22}$$

2.2. Determination of temperature distribution

In view of the miniature size of the sample, the temperature distribution is determined indirectly. Temperature distribution is determined based on FEM modelling of the process, assuming (23). Information on boundary conditions and verification of modelling results is provided by the temperature measurement devices. It is understood that by combining (15) and (23), the dependence $\sigma_H(T)$ (MPa) can be determined, which is the goal.

$$T_M(h) = T_R(h) \tag{23}$$

3. FEM MODELING

An important element of the method is the FEM modelling leading to determine the temperature distribution in the volume of a deformed micro-sample. This distribution has a key impact on the final results of the study. It is determined on the basis of records of the course of temperatures collected from the surface of the matrix by a pyrometer, the interior of the fitting by a thermocouple and the surface of the stamp holder also by a thermocouple. The cooling water temperature is also taken into account. Modelling is carried out using the MS Marc-Mentat 2015 package in the "thermal / structural" analysis in a static model with a deformed material model taking into account the dependence of the yield stress on the deformation and temperature. The results for the analysed case are shown in **Figure 3**.

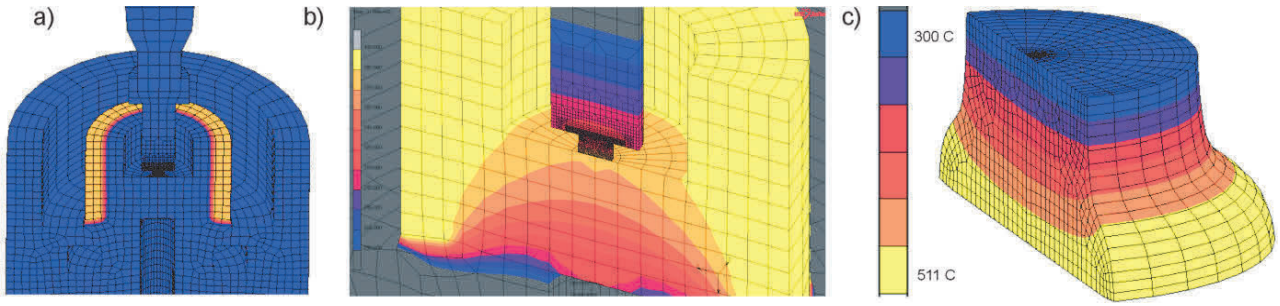

Figure 3 Examples of temperature distributions obtained in FEM modelling: a) initial and boundary conditions of induction heating, b) medium phase of deformation, c) sample in the final state of deformation

4. EXPERIMENT RESULTS

The MUNUT process was applied to the cylindrical sample made of Bulk Metallic Glass based on copper, zirconium, titanium and silver. The sample diameter is 1.2 mm and the height is 1 mm - see **Figure 2d**. Sample was upsetted to the height of h_1 = 0.68 mm - see **Figure 2e**.

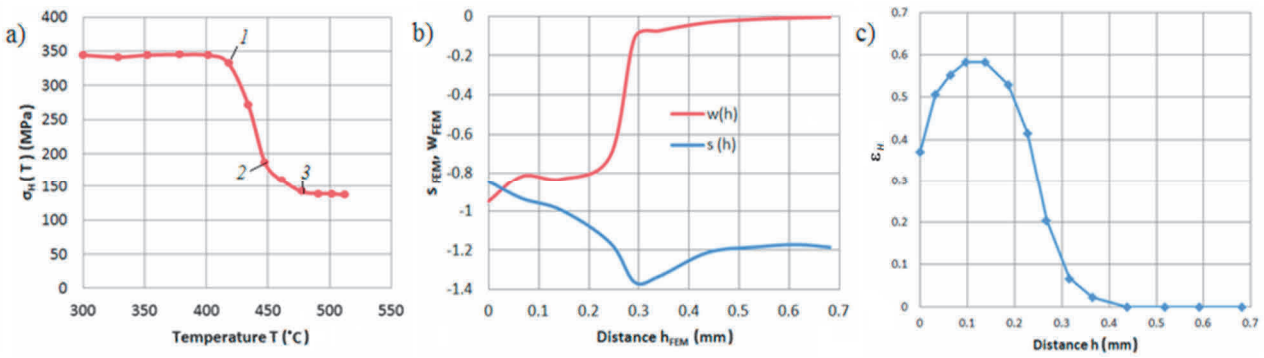

Figure 4 Test results: a) distribution of yield stress as a function of temperature, b) distributions of proportionality function, c) distribution of equivalent strain in a sample

The sample was deformed at the ram rate of 0.1 mm / min, which means in the applied upset range the strain rate 1.6 - 2.2 e-3 s^{-1}. As a result of the applied method, the distribution of yield stress was obtained from the temperature in the test range, i.e. from 300 to 511 °C. This distribution is shown in **Figure 4a**. This figure also shows the distributions of the stress and strain proportionality functions, **Figure 4b** and the distribution of the equivalent strain, **Figure 4c**.

5. DISCUSSION AND CONCLUSIONS

The yield stress of investigated BMG is clearly falling near the temperature of 430 °C, point 1 in **Figure 4a**. This drop decreases its intensity in the range of 450 - 470 °C, between points 2 and 3. Above 470 °C, point 3, it stabilizes. From the course it follows that the temperature of transition into a supercooled liquid state is in the range of 450 - 470 °C. More precisely, it can be determined by concentrating the number of points analyzed in an interesting range. The obtained result is consistent with the one awaited, because according to the literature of this type, metallic glasses have the temperature of transition just in this range. The proposed MUNUT method allows the determination of temperature-dependent plastic properties of the material under plastic microforming conditions on the basis of a single experiment. The following conclusions might be stated:

- The accuracy of the MUNUT method depends on the accuracy of determining the temperature distribution in the upset sample, and on the number of cross-sections considered.
- The obtained results may be influenced by friction occurring on the sample and tool contact surfaces, hence it is recommended to upset at the lowest possible friction.
- A method has been piloted and successfully used to determine the liquid transition temperature range of bulc metallic glass in the microforming conditions.
- The obtained glass transition temperature range of the tested material is in accordance with literature data.

Further development of the method provides for CCD camera recording of the lateral view of the upset micro-sample and analysis of a number of deformation states.

ACKNOWLEDGEMENTS

The sample of the MUNUT method used was a sample of metallic glass designed and made under the direction of prof. dr hab. Eng. Tadeusz Kulik, Warsaw Univ. of Technology. This work is partially supported (UMO-2011/01 / B / ST8 / 07731) by the National Science Centre.

REFERENCES

[1] SANTOME, Y. and IWAZAKI, H. Superplastic backward microextrusion of microparts for micro-electro-mechanical systems. *Journal of Materials Processing Technology*. 2001. vol. 119, pp. 307-311.

[2] GEIGER, M., KLEINER, M., ECKSTEIN, R., TIESLER, N. AND ENGEL, U. Microforming. *CIRP Annals - Manufacturing Technology*. 2001. vol. 50, no. 2, pp. 445-462.

[3] GEIGER, M., ENGEL U., VOLLERTSEN, F., KALS, R. and MESSNER, A. Metal forming of micro parts for electronics. *Production engineering*. 1994. vol. 2, no. 1, pp. 15-18.

[4] MOLOTNIKOW, A., LAPOVOK, R., GU, C.F., DAVIES, C.H.J. and ESTRIN, Y. Size effects in micro cup drawing. *Materials Science and Engineering: A*. 2012. vol. 550. pp. 312-319.

[5] RAULEA, L.V., GOIJAERTS, A.M., GOVAERT, L.E. and BAAIJENS, F.P.T. Size effect in the processing of thin metal sheets. *Journal of Materials Processing Technology*. 2001. vol. 115, pp. 44-48.

[6] RAN, J.Q., FU, M.W. and CHAN, W.L. The influence of size effect on the ductile fracture in micro-scaled plastic deformation. *International Journal of Plasticity*. 2013. vol. 41, pp. 65-81.

[7] PRESZ, W. Scale effect in design of the pre-stressed micro-dies for microforming. *Computer Methods in Material Science.* 2016. vol. 16, no. 4, pp.196-203.

[8] CANNELLA, E., NIELSEN, E.K. and STOLFI, A. Designing a Tool System for Lowering Friction during the Ejection of In-Die Sintered Micro Gears. *Micromachines.* 2017. vol. 8, no. 7, pp. 214-229.

[9] PRESZ, W. Dynamic effect in ultrasonic assisted micro-upsetting. In *ESAFORM 2018:* 21st International ESAFORM Conference on Material Forming. AIP Conference Proceedings. 2018. vol. 1960, no. 1, p. 100012.

[10] STELLIN, T., TIJUM, R. and ENGEL, U. Modelling and experimental study of a microforging process from metal strip for the reduction of defects in mass production. *Production Engineering.* 2016. vol.10., no. 2, pp.103-112.

[11] WANG, C., GUO, B., SHAN, D., ZHANG, M. and BAI, X. Tribological behaviours in microforming considering microscopically trapped lubricant at contact interface. *The Int. J. of Advanced Manufacturing Technology*. 2014. vol. 71, no. 9-12, pp. 2083-2090.

[12] SHIMIZU, T. KAKEGAWA, T. and YANG, M. Micro-texturing of DLC thin film coatings and its tribological performance under dry sliding friction for microforming operation. *Procedia Eng.* . 2014. vol. 81, pp. 1884-1889.

[13] WANG, D., SHI, T., PAN, J., LIAO, G., TANG, Z. and LIU, L. Finite element simulation and experimental investigation of forming micro-gear with Zr-Cu-Ni-Al bulk metallic glass. *Journal of Materials Processing Technology*. 2010. vol. 210, no. 4, pp. 684-688.

[14] KOCANDA, A., PRESZ, W, ADAMCZYK, G., CZYZEWSKI, P. and MAZUREK, W. Contact pressure distribution in upsetting of compound metals. *Journal of Material Processing Technology*. 1996. vol. 60, no. 1-4, pp. 343-348.

[15] MA, J., GONG, F., YANG, Z. and ZENG, W.Q. Microdeep drawing of C1100 microsquare cups using microforming technology. *International Journal of Advanced Manufacturing Technology*. 2016. vol. 82, no. 5-8, pp.1363-1369.

[16] GHASSEMALI, E., TAN, M.J., WAH, C.B., JARFORS, A.E.W. and LIM, S.C.V. Grain size and workpiece dimension effects on material flow in an open-die micro-forging/extrusion process. *Material Science and Engineering: A*. 2013. vol. 582, pp. 379-388.